Features of blast wave energy dissipation using aqueous foam

© R.Kh. Bolotnova, E.F. Gainullina, V.A. Korobchinskaya

Mavlyutov Institute of Mechanics UFRC RAS, Ufa, Russia
E-mail: elina.gef@yandex.ru

Received May 12, 2023
Revised September 29, 2023
Accepted October, 30, 2023

Dynamics features of the shock waves arising from the explosion of a cylindrical high explosive (HE) in air and aqueous foam layer surrounding the charge are studied on the basis of a two-phase gas-liquid model in one-pressure, two-velocity, two-temperature approximations, taking into account the interfacial interaction forces and interfacial heat transfer processes. Based on the results of the research, the degree of reduction in the speed and amplitude of the shock pulse in the presence of aqueous foam layer was estimated in comparison with the air medium. A comparative analysis of the obtained calculations with experimental data is carried out. The safe distance for a human from the explosion center in the air and with the use of a protective aqueous foam barrier was estimated.

Keywords: explosion of cylindrical form HE, air medium, aqueous foam, shock waves, numerical simulation.

DOI: 10.61011/TPL.2023.12.57600.106A

The study of shock wave (SW) attenuation through the use of aqueous foam is important from the point of view of analyzing the effectiveness of foam barriers in shock protection applications. The results of a series of field experiments on the detonation of an explosive charge in gas and water foam show a significant reduction in the intensity of the impact when the explosive charge is surrounded by foam [1–3]. A study of the dynamics of weak SW using shock tubes containing gas and a layer of aqueous foam showed a significant decrease in the velocity of the compression wave during its propagation in the foam medium [4,5].

Mathematical models describing shock-wave processes in aqueous foam are proposed in [6–8]. On the basis of the two-phase gas-drop model in [6], the peculiarities of the dynamics of a spherical explosion in foam are studied for the conditions of the experiments described in [1], and the modelling problem of the interaction of an air spherical pressure pulse with the foam layer is solved [7]. In [8], an elastic-viscoplastic model of foam has been developed to describe its behavior under weak impact. The process of elastic precursor formation ahead of the main compression wave is analyzed. Further studies aimed at a more detailed study of the effectiveness of the foam barrier surrounding the explosive charge are of interest.

In the present work, the dynamics of strong SW in air and water foam is investigated for the conditions of field experiments [3] in which a cylindrically shaped explosive charge was surrounded by a hemispherical layer of water foam. In contrast to the experiments [1] on high explosive (HE) spherical explosion with energy $\Delta E \approx 7.7 \cdot 10^5$ J in a vessel of volume $V \approx 8\,\text{m}^3$, completely filled with aqueous foam, in the experiments considered in this work [3] the explosive charge was covered with a foam layer of small thickness with a total volume $V \approx 1\,\text{m}^3$.

The scheme of the experiment presented in [3] is shown in Fig. 1. A cylindrical explosive charge C4 of mass $M_{HE} = 82\,\text{g}$ with energy $\Delta E \approx 4.2 \cdot 10^5$ J was placed on a metal plate of diameter $d = 0.76\,\text{m}$. The pressure sensor was fixed at a distance $l = 0.5\,\text{m}$ and height $h = 0.23\,\text{m}$ relative to the explosive charge so that the reflected waves would not affect the measurement results. At the first stage of experiments the HE explosion in air was investigated, at the second stage the charge was surrounded by a hemispherical layer of water foam with radius $r_{foam} = 0.2\,\text{m}$ and density $\rho_{foam} \approx 60\,\text{kg/m}^3$, which corresponds to the foam with initial volume water content $\alpha_{10} \approx 6\%$.

The process of propagation of strong SW in air and water foam was described by the model of two-phase gas-liquid medium with individual distributions of velocities and temperatures of phases under the assumption of equality of phase pressures [9,10]. Next, the conservation equations of

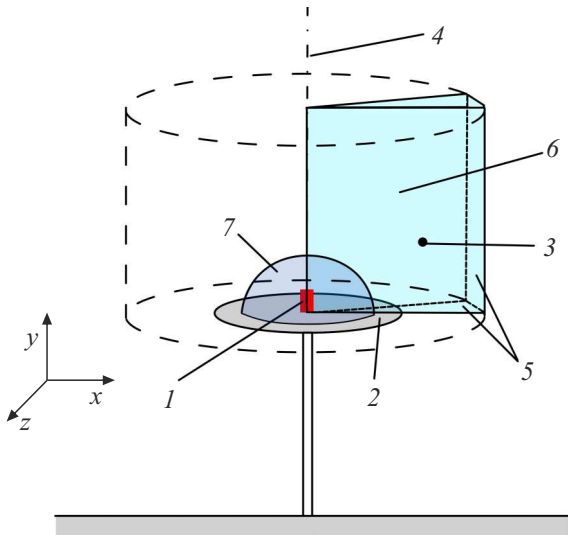

Figure 1. Scheme of the experiment [3] and computational domain. *1* — explosive charge, *2* — rigid surface, *3* — pressure sensor, *4* — symmetry axis, *5* — free boundaries, *6* — computational domain, *7* — water foam layer.

mass, momentum, energy of i-phase and the equation of dynamics of volume water content are given:

$$\frac{\partial(\alpha_i\rho_i)}{\partial t} + \mathrm{div}(\alpha_i\rho_i\mathbf{v}_i) = 0, \quad (1)$$

$$\frac{\partial(\alpha_i\rho_i\mathbf{v}_i)}{\partial t} + \mathrm{div}(\alpha_i\rho_i\mathbf{v}_i\mathbf{v}_i) = -\alpha_i\nabla p + \mathrm{div}(\alpha_i\tau_i) + \mathbf{F}_{i,drag} + \mathbf{F}_{i,vm}, \quad (2)$$

$$\frac{\partial\big(\alpha_i\rho_i(e_i+K_i)\big)}{\partial t} + \mathrm{div}\big(\alpha_i\rho_i(e_i+K_i)\mathbf{v}_i\big) = -p\frac{\partial\alpha_i}{\partial t} - \mathrm{div}(\alpha_i\mathbf{v}_i p) + \mathrm{div}\left(\alpha_i\frac{c_{p,i}}{c_{V,i}}\gamma_i\nabla h_i\right) + K_{ht}(T_j - T_i), \quad (3)$$

$$\frac{\partial\alpha_1}{\partial t} + \mathrm{div}(\alpha_1\mathbf{v}) + \mathrm{div}\big(\alpha_1\alpha_2(\mathbf{v}_1-\mathbf{v}_2)\big) - \alpha_1\mathrm{div}\mathbf{v} = \alpha_1\alpha_2\left(\frac{1}{\rho_2}\frac{d\rho_2}{dt} - \frac{1}{\rho_1}\frac{d\rho_1}{dt}\right). \quad (4)$$

In equations (1)–(4), the following notations are used: α_i — volume content, ρ_i — density, $\mathbf{v}_i$ — velocity, γ_i — diffusivity, T_i — temperature, p — pressure, K_i — kinetic energy, $c_{p,i}$, $c_{V,i}$ — specific heat capacities at constant pressure and volume, K_{ht} — heat transfer coefficient, h_i — enthalpy, $\mathbf{v} = \alpha_1\mathbf{v}_1 + \alpha_2\mathbf{v}_2$ — velocity of the gas-liquid mixture. The lower indices $i, j = 1, 2$ denote the aqueous and gas phases of the foam.

In equation (2), the viscous stress tensor and the force of attached masses have the form

$$\tau_i = \mu_i\big(\nabla\mathbf{v}_i + \nabla\mathbf{v}_i^T\big) - \frac{2}{3}\big(\mu_i\mathrm{div}\mathbf{v}_i\big)\mathbf{I},$$

$$\mathbf{F}_{i,vm} = 0.5\alpha_1\rho_2\left(\frac{d_i\mathbf{v}_i}{dt} - \frac{d_j\mathbf{v}_j}{dt}\right),$$

where μ_i — dynamic viscosity, $\mathbf{I}$ — unit tensor. The Schiller–Naumann model was chosen to describe the interfacial resistance in a gas-droplet medium with droplet diameter d_{10}

$$\mathbf{F}_{i,drag} = \frac{3}{4}\alpha_1 C_D\frac{\rho_2}{d_{10}}\big(\mathbf{v}_i - \mathbf{v}_j\big)\big|\mathbf{v}_i - \mathbf{v}_j\big|.$$

Interfacial heat transfer was accounted for according to the Ranz–Marshall model

$$K_{ht} = \frac{\kappa_2}{d_{10}}\mathrm{Nu}, \quad \mathrm{Nu} = 2 + 0.6\mathrm{Re}^{1/2}\mathrm{Pr}^{1/3},$$

κ_2 — thermal conductivity of air, Nu, Pr — Nusselt and Prandtl numbers. The properties of air and water are described by perfect equations of state according to [11]. The numerical implementation of the model was performed in the OpenFOAM [11] software package.

A gas-drop model was used to describe the behavior of aqueous foam, which assumes that strong SW impact SW destroys the foam structure by forming a suspension of microdroplets [1] behind the SW front. It is assumed that at temperatures above critical values, droplet vaporization occurs behind the SW front, which is accompanied by the transition of the gas-drop mixture into a single-phase gas medium with a significant loss of SW energy (up to 80%).

The axisymmetric approximation was used in numerical modelling of the investigated process. The computational domain was constructed according to the experimental data [3] (Fig. 1) under the following boundary conditions: Oy — symmetry axis; $0 \leqslant x \leqslant 0.38$, $y = 0$ [m] — rigid wall defining the presence of a rigid surface *2*; on the remaining surfaces, the free boundary condition is specified. The explosion was modelled as an initial pulse

$$p(0,x,y,z) = p_0 + \Delta p\exp\big(-(x^2+y^2+z^2)/a^2\big),$$

$$T(0,x,y,z) = T_0 + \Delta T\exp\big(-(x^2+y^2+z^2)/a^2\big), \quad (5)$$

where a — pulse width, p_0, T_0 — pressure and temperature of undisturbed medium, Δp, ΔT — maximum amplitudes of overpressure and temperature. The parameters of the initial pulse (5) were chosen in such a way that in the process of calculations the formed SW coincided with its experimental profile (Fig. 2) on the pressure sensor *3* [3].

To substantiate the validity of numerical modelling, a comparison of calculated and experimental pressure oscillograms at the sensor location *3* (Fig. 1) is presented in Fig. 2 for HE explosion in air (a) and when the explosive charge is surrounded by water foam (b). A satisfactory agreement between the calculations and the experimental data [3] is obtained. The data of calculations and experiments presented in Fig. 2 show that the application of water foam reduces the front velocity and amplitude of the formed SW at the sensor *3* by ~ 43 and ~ 70%, respectively.

Fig. 3 shows the spatial dynamics of SW resulting from the explosion of a cylindrical charge in air (a) and water foam (b) for the time moments $t = 0.25$ and 0.4 ms, corresponding to the time of SW arrival at the sensor (compare with Fig. 2). The wave flow pattern obtained in the calculations in the form of pressure field distribution qualitatively and in form agrees with the numerical solutions presented in [3] for the experimental conditions with more powerful explosion energy in the air $\Delta E \approx 1.3\cdot 10^6$ J of a cylindrically shaped explosive charge.

As a result of our calculations, it was found that in the presence of a foam barrier, the emerging mode of wave flow is characterized by a significant dissipation of the explosion energy at the initial stage of the SW interaction process with water foam due to the loss of energy for evaporation of the water phase in the central high-temperature zone of the explosion, which weakens the explosion energy more than 4 times. A comparative analysis of numerical solutions obtained for the HE explosion in the presence of the water foam layer and without it has shown that the maximum values of pressure and velocities are observed at the SW front near the $y = 0$ axis, while behind the SW front in the central region near the

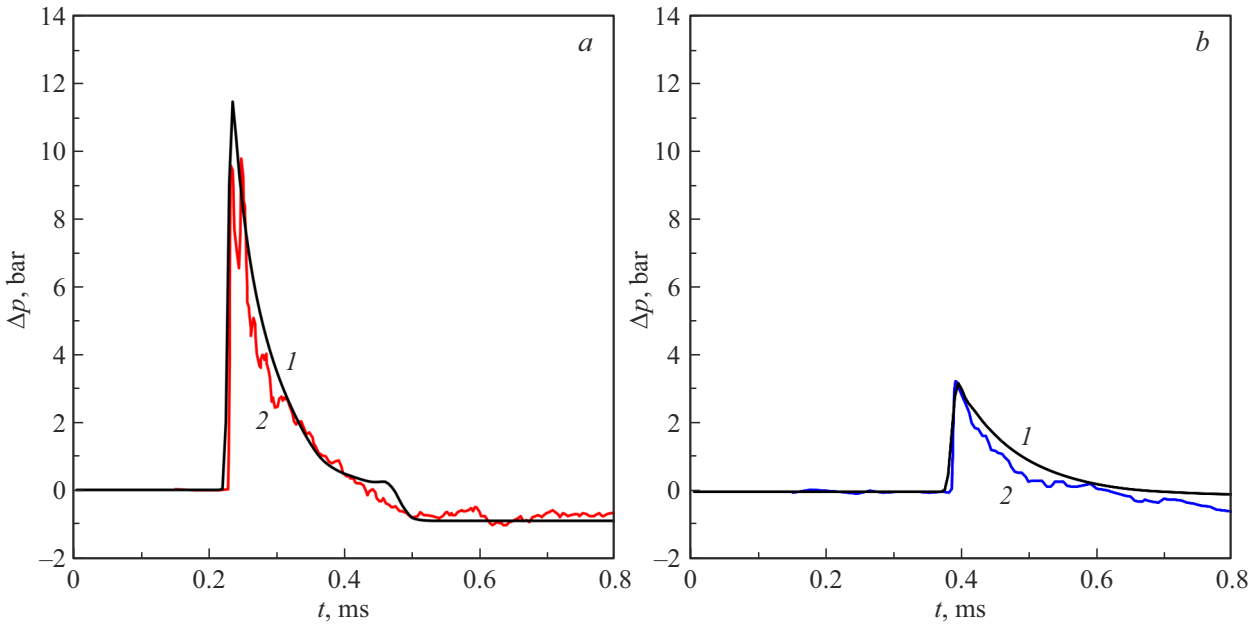

Figure 2. Calculated (*1*) and experimental (*2*) pressure oscillograms at the sensor location at a distance $l = 0.5$ m [3] from the center of the HE explosion: in air (*a*) and when the explosive charge is surrounded by a layer of water foam (*b*).

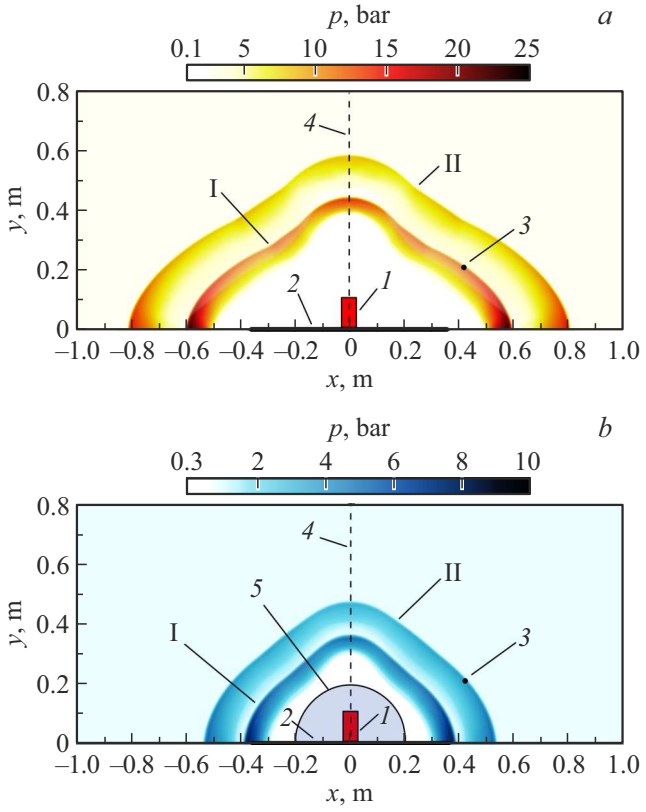

Figure 3. Calculated pressure field distributions for explosion in air (*a*) and for surrounding the explosive charge with a layer of water foam (*b*) [3] at time $t = 0.25$ (I) and 0.4 ms (II). *1* — charge explosive at time $t = 0$, *2* — rigid surface, *3* — pressure sensor, *4* — symmetry axis, *5* — water foam layer at time $t = 0$.

symmetry axis, a rarefaction zone expanding with time is formed.

Research [12] provides data on the effects of shock on humans. It is shown that an overpressure pulse of amplitude $\Delta p > 0.34$ bar leads to rupture of the tympanic membrane; explosive lung damage occurs at $\Delta p > 1$ bar. Consequently, based on the data [12], in the case of the experiment under study on the HE explosion in air with energy $\Delta E \approx 4.2 \cdot 10^5$ J the minimum safe distance from the center of the explosion for a human is $l_{safe} \approx 2.5$ m, where $\Delta p < 0.3$ bar. When the explosive charge is surrounded by a layer of water foam with a thickness of $r_{foam} = 0.2$ m due to the weakening effect of the foam l_{safe} is reduced by a factor of ~ 1.7 times and is ~ 1.5 m.

Thus, the use of foam barriers is able to protect a person from the destructive impact of the HE explosion, which can be used in solving the problems of ensuring safety in emergency situations.

Funding

The research was financially supported by the state budget under the state task 0246-2019-0052.

Conflict of interest

The authors declare that they have no conflict of interest.

References

[1] E. Del Prete, A. Chinnayya, L. Domergue, A. Hadjadj, J.-F. Haas, Shock Waves, **23** (1), 39 (2013). DOI: 10.1007/s00193-012-0400-0

[2] K.L. Monson, K.M. Kyllonen, J.L. Leggitt, K.E. Edmiston, C.R. Justus, M.F. Kavlick, M. Phillip, M.A. Roberts, C.W. Shegogue, G.D. Watts, J. Forensic Sci., **65** (6), 1894 (2020). DOI: 10.1111/1556-4029.14536
[3] K. Ahmed, A.Q. Malik, AIP Adv., **10** (6), 065130 (2020). DOI: 10.1063/5.0010283
[4] M. Monloubou, J. Le Clanche, S. Kerampran, in *Actes 24ème Congrès Français de Mécanique* (Association Française de Mécanique, Brest, 2019), p. 255125.
[5] S.P. Medvedev, S.V. Khomik, V.N. Mikhalkin, A.N. Ivantsov, G.L. Agafonov, A.A. Cherepanov, T.T. Cherepanova, A.S. Betev, J. Phys.: Conf. Ser., **946**, 012061 (2018). DOI: :10.1088/1742-6596/946/1/012061
[6] R.Kh. Bolotnova, E.F. Gainullina, Fluid Dyn., **55** (5), 604 (2020). DOI: 10.1134/S001546282005002X.
[7] R.Kh. Bolotnova, E.F. Gainullina, J. Phys.: Conf. Ser., **1268**, 012015 (2019). DOI: 10.1088/1742-6596/1268/1/012015
[8] R.Kh. Bolotnova, E.F. Gainullina, J. Phys.: Conf. Ser., **2103**, 012217 (2021). DOI: 10.1088/1742-6596/2103/1/012217
[9] R.I. Nigmatulin, *Dynamics of multiphase media* (Hemisphere, N.Y., 1990).
[10] L.D. Landau, E.M. Lifshitz, *Fluid mechanics* (Pergamon Press, Oxford, 1987), vol. 6.
[11] *OpenFOAM. The open source computational fluid dynamics (CFD) toolbox* [Electronic source]. http://www.openfoam.com
[12] P. Peters, Mil. Med., **176** (1), 110 (2011). DOI: 10.7205/milmed-d-10-00300

Translated by J.Deineka